

# Kondo effect induced by a magnetic field

M. Pustilnik and L. I. Glazman

*Theoretical Physics Institute, University of Minnesota,  
116 Church St. SE, Minneapolis, MN 55455*

We study peculiarities of transport through a Coulomb blockade system tuned to the vicinity of the spin transition in its ground state. Such transitions can be induced in practice by application of a magnetic field. Tunneling of electrons between the dot and leads mixes the states belonging to the ground state manifold of the dot. Remarkably, both the orbital and spin degrees of freedom of the electrons are engaged in the mixing at the singlet-triplet transition point. We present a model which provides an adequate theoretical description of recent experiments with semiconductor quantum dots and carbon nanotubes.

PACS numbers: 72.15.Qm, 73.23.Hk, 73.40.Gk, 85.30.Vw

## I. INTRODUCTION

Quantum dot devices provide a well-controlled object for studying quantum many-body physics. In many respects, such a device resembles an atom imbedded into a Fermi sea of itinerant electrons. These electrons are provided by the leads attached to the dot. The orbital mixing in the case of quantum dot corresponds to the electron tunneling through the junctions connecting the dot with leads. Voltage  $V_g$  applied to a gate – an electrode coupled to the dot capacitively – allows one to control the number of electrons  $N$  on the dot. Almost at any gate voltage an electron must have a finite energy in order to overcome the on-dot Coulomb repulsion and tunnel into the dot. Therefore, the conductance of the device is suppressed at low temperatures (Coulomb blockade phenomenon [1]). The exceptions are the points of charge degeneracy. At these points, two charge states of the dot have the same energy, and an electron can hop on and off the dot without paying an energy penalty. This results in a periodic peak structure in the dependence of the conductance  $G$  on  $V_g$ . Away from the peaks, in the Coulomb blockade valleys, the charge fluctuations are negligible, and the number of electrons  $N$  is integer.

Every time  $N$  is tuned to an odd integer, the dot must carry a half-integer spin. In the simplest case, the spin is  $S = 1/2$ , and is due to a single electron residing on the last occupied discrete level of the dot. Thus, the quantum dot behaves as  $S = 1/2$  magnetic impurity imbedded into a tunneling barrier between two massive conductors. It is known [2] since mid-60's that the presence of such impurities leads to zero-bias anomalies in tunneling conductance [3], which are adequately explained [4] in the context of the Kondo effect [5]. The advantage of the new experiments [6] is in full control over the “magnetic impurity” responsible for the effect. For example, by varying the gate voltage,  $N$  can be changed. Kondo effect results in the increased low temperature conductance only in the odd- $N$  valleys. The even- $N$  valleys nominally correspond to the  $S = 0$  spin state (non-magnetic impu-

rity), and the conductance decreases with lowering the temperature.

However, the enhancement of the low temperature conductance in the even- $N$  valleys has been observed recently in both vertical [7] and lateral [8] GaAs quantum dots, and in transport through carbon nanotubes [9]. Unlike the real atoms, the energy separation between the discrete states in a quantum dot is fairly small. Therefore, the  $S = 0$  state of a dot with even number of electrons is less robust than the corresponding ground state of a real atom. Because of the exchange interactions between electrons residing on the last doubly occupied level, one of the electrons is promoted to the next (empty) orbital state, and thus a triplet spin state of the dot is formed. Apparently, dots studied in [7] and [8] were in a triplet state in the absence of magnetic field. On the other hand, experiments with carbon nanotubes [9] indicate that in the absence of magnetic field the state with even number of electrons is a singlet.

Application of a magnetic field results in a spin transition in the ground state of a quantum dot [7] or carbon nanotube [9]. In the former case the Zeeman effect is negligible because of the small  $g$ -factor in GaAs; magnetic field affects mostly the orbital states, making energy of the triplet state higher than that of the singlet. In the latter case, the Zeeman contribution dominates and can exceed the level spacing, i.e., the magnetic field induces the transition to a triplet state. Electron tunneling between the dot and leads results in mixing of the components of the ground state. The mixing involves spin as well as orbital degrees of freedom and yields an enhancement of the low temperature conductance through the dot at the transition point. This enhancement can be viewed as a *magnetic field-induced Kondo effect* [10].

In Section II a simple model capable of describing the singlet-triplet transition in Coulomb blockade systems is introduced. In Section III we derive an effective low energy Hamiltonian and establish the Fermi-liquid nature of its ground state. The Hamiltonian is analyzed by means of renormalization group in Sections IV-VI. Generaliza-

tions of the model are discussed in Appendices C-E.

Section V is relevant for the experiments [7] with vertical GaAs quantum dots. In this case the Zeeman energy is very small due to an anomalously small electronic  $g$ -factor in GaAs. The low energy physics in this limit is described by a special version of a two-impurity Kondo model [11]. We show that at zero temperature the linear DC conductance is a monotonous function of a magnetic field, reaching the unitary limit  $\sim 4e^2/h$  at the triplet side of the singlet-triplet transition, and decreasing logarithmically at the singlet side. The Kondo temperature on the triplet side of the transition falls off rapidly from  $T_0$  at the transition point down to  $T_K^{\text{triplet}}$  far away from the transition [11–13].

The relations between  $T_0$ ,  $T_K^{\text{triplet}}$ , and the Kondo temperature  $T_K^{\text{odd}}$  in the adjacent Coulomb blockade valleys depend on the tunneling amplitudes between the dot and the leads and also on the intradot interactions. If the tunneling preserves the orbital symmetry, as it likely occurs in vertical quantum dots [7,14], then  $T_K^{\text{triplet}} \ll T_K^{\text{odd}} \lesssim T_0$ . Accordingly, at a finite temperature  $T_K^{\text{triplet}} \ll T \lesssim T_0$  the Kondo effect in  $N = \text{even}$  valley of Coulomb blockade can be observed only when the system is tuned to the singlet-triplet transition point [7].

If the tunneling mixes the orbitals, the difference between  $T_K^{\text{triplet}}$  and  $T_K^{\text{odd}}$  becomes less pronounced and vanishes if the mixing is strong, see Appendix D. The relation between  $T_0$  and  $T_K^{\text{odd}}$  is almost independent on the degree of mixing but depends strongly on the intradot interactions, see Appendices C,D.

In Section VI we discuss the Zeeman splitting-driven transition [15], relevant for the transport experiments with carbon nanotubes [9]. In this system, the  $g$ -factor is close to its free-electron value, while the orbital effects are suppressed due to a small radius of the nanotube. The low energy physics in this case is described adequately by the single-channel anisotropic Kondo model. Tuning away from the transition points is equivalent to applying a finite magnetic field to the conventional Kondo impurity. The DC conductance has a peak at the transition point at all values of  $T$ , with the corresponding Kondo temperature being of the same order as  $T_K^{\text{odd}}$ .

Finally, in Section VII we demonstrate that in a generic case the positions of the peaks of *non-linear* conductance are not symmetric with respect to the change of the bias polarity. This effect is weak and can be best seen in double-dot systems.

## II. THE MODEL

We will consider a confined electron system which does not have special symmetries, and therefore the single particle levels in it are non-degenerate. In addition, we

assume the electron-electron interaction to be relatively weak (the gas parameter  $r_s \lesssim 1$ ). Therefore, discussing the ground state, we concentrate on the transitions which involve only the lowest-spin states. In the case of *even* number of electrons  $N$  on the dot, these are states with  $S = 0$  and  $S = 1$ . At a sufficiently large level spacing  $\delta \equiv \epsilon_{+1} - \epsilon_{-1}$  between the last occupied ( $-1$ ) and the first empty orbital level ( $+1$ ), the ground state is a singlet at  $B = 0$ . Finite magnetic field affects the orbital energies; if it reduces the difference between the energies of the said orbital levels, a transition to a state with  $S = 1$  may occur, as illustrated at Fig. 1. Such a transition involves rearrangement of two electrons between the levels  $n = \pm 1$ . Out of the six states involved, three belong to a triplet  $S = 1$ , and three others are singlets ( $S = 0$ ). The degeneracy of the triplet states is removed only by Zeeman energy. The three singlet states, in general, are not degenerate with each other. To describe qualitatively the transition between a singlet and the triplet in the ground state, it is sufficient to consider the following Hamiltonian:

$$H_{\text{dot}} = \sum_{ns} \epsilon_n d_{ns}^\dagger d_{ns} - E_S \mathbf{S}^2 - E_Z S^z + E_C (N - \mathcal{N})^2. \quad (1)$$

Here,  $N = \sum_{s,n} d_{ns}^\dagger d_{ns}$  is the total number of electrons occupying the levels  $n = \pm 1$ , operator

$$\mathbf{S} = \sum_{nss'} d_{ns}^\dagger \frac{\boldsymbol{\sigma}_{ss'}}{2} d_{ns'}$$

is the corresponding total spin of the dot ( $\boldsymbol{\sigma}$  are the Pauli matrices), and the parameters  $E_S$ ,  $E_C$ , and

$$E_Z = g_d \mu_B B, \quad (2)$$

are the exchange, charging, and Zeeman energies respectively [16]. We restrict our attention to the very middle of a Coulomb blockade valley with an even number of electrons in the dot (that is modelled by setting the dimensionless gate voltage  $\mathcal{N}$  to  $\mathcal{N} = 2$ ). We assume that the level spacing  $\delta$  is tunable, *e.g.*, by means of a magnetic field  $B$ :  $\delta = \delta(B)$ .

The lowest energy singlet state and the three components of the competing triplet state can be labeled as  $|S, S^z\rangle$  in terms of the total spin  $S$  and its  $z$ -projection  $S^z$ ,

$$\begin{aligned} |1, 1\rangle &= d_{+1\uparrow}^\dagger d_{-1\uparrow}^\dagger |0\rangle, \\ |1, -1\rangle &= d_{+1\downarrow}^\dagger d_{-1\downarrow}^\dagger |0\rangle, \\ |1, 0\rangle &= \frac{1}{\sqrt{2}} \left( d_{+1\uparrow}^\dagger d_{-1\downarrow}^\dagger + d_{+1\downarrow}^\dagger d_{-1\uparrow}^\dagger \right) |0\rangle, \\ |0, 0\rangle &= d_{-1\uparrow}^\dagger d_{-1\downarrow}^\dagger |0\rangle, \end{aligned} \quad (3)$$

where  $|0\rangle$  is the state with the two levels empty. From (1), the energies of these states satisfy

$$E_{|S,S^z\rangle} - E_{|0,0\rangle} = K_0 S - E_Z S^z, \quad K_0 = \delta - 2E_S \quad (4)$$

If, for example,  $K_0 > 0$  at  $B = 0$ , the ground state of the dot in the absence of the magnetic field is a singlet  $|0,0\rangle$ . Finite field shifts the singlet and triplet states due to the orbital effect, and also leads to Zeeman splitting of the components of the triplet. As  $B$  is varied, the level crossings occur (see Fig. 1). The first such crossing takes place at  $B = B^*$ , for which

$$\Delta = E_{|0,0\rangle} - E_{|1,1\rangle} = 0. \quad (5)$$

At this point the two states,  $|1,1\rangle$  and  $|0,0\rangle$ , form a doubly degenerate ground state of the dot.

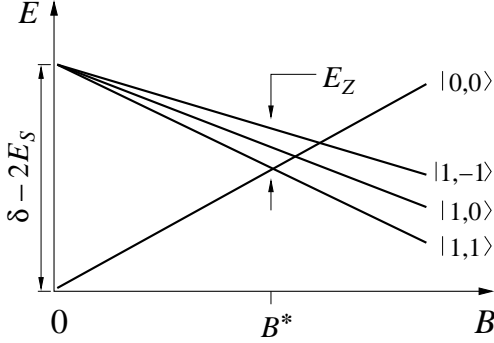


FIG. 1. Typical picture of the singlet-triplet transition in the ground state of a quantum dot.

If leads are attached to the dot, the dot-lead tunneling results in the hybridization of the degenerate (singlet and triplet) states. The characteristic energy scale  $T_0$  associated with the hybridization can be in different relations with the Zeeman splitting at field  $B = B^*$ .

If  $E_Z(B^*) \ll T_0$ , then the Zeeman splitting can be neglected, and at the  $B = B^*$  point all *four* states (3) can be considered as degenerate. This limit adequately describes a quantum dot formed in a two-dimensional electron gas (2DEG) at the GaAs-AlGaAs interface, subject to a magnetic field [7,14]. Indeed, the orbital effect of a magnetic field is very strong in GaAs due to a smallness of the effective mass, so that a relatively weak magnetic field  $B^*$  suffices to induce the spin transition. In addition, the electronic  $g$ -factor in GaAs is also small. Both these factors contribute to the smallness of the Zeeman energy  $E_Z(B^*) = g_d \mu_B B^*$  compared to  $T_0$ . This case is studied in details in Section V.

The opposite limit  $E_Z(B^*) \gg T_0$  is realized in carbon nanotubes [9]. In nanotubes, on the one hand, the effect of magnetic field on orbital motion is very weak due to their small diameter. On the other hand, the  $g$ -factor is close to its free electron value  $g = 2$ , yielding an appreciable Zeeman splitting even in a magnetic field of moderate strength. This limit of the theory is addressed in Section VI.

In order to study the transport problem, we need to introduce into the model the Hamiltonian of the leads and

a term that describes the tunneling. We choose them in the following form:

$$H_l = \sum_{\alpha n k s} \xi_{ks} c_{\alpha n k s}^\dagger c_{\alpha n k s}, \quad \xi_{ks} = \xi_k - \frac{s}{2} g_c \mu_B B \quad (6)$$

$$H_T = \sum_{\alpha n n' k s} t_{\alpha n n'} c_{\alpha n k s}^\dagger d_{n' s} + \text{H.c.} \quad (7)$$

Here  $\alpha = R, L$  for the right/left lead, and  $n = \pm 1$  for the two orbitals participating in the singlet-triplet transition;  $k$  labels states of the continuum spectrum in the leads, and  $s = \pm 1$  is the spin index. The single-particle energies  $\xi_{ks}$  include the direct effect of the external magnetic field on the electrons in the leads.

In writing (6)-(7), we had in mind the vertical dot device [7], where the potential creating lateral confinement of electrons most probably does not vary much over the thickness of the dot [14]. Therefore we have assumed that the electron orbital motion perpendicular to the axis of the device can be characterized by the same quantum number  $n$  inside the dot and in the leads. Presence of two orbital channels  $n = \pm 1$  is important for the explanation of experiments [7], in which the orbital effect of the magnetic field dominates. In the case of large Zeeman splitting, the problem effectively becomes a single-channel one [15], as we will see in Section VI.

### III. LOW ENERGY HAMILTONIAN

We will demonstrate the derivation of the effective low energy Hamiltonian under a simplifying assumption [11,12]

$$t_{\alpha n n'} = t_\alpha \delta_{n n'}. \quad (8)$$

It has been shown previously [10] that, despite its simplicity, Eq. (8) still allows to understand, at least qualitatively, the most interesting results of the experiments [7,9]. Some of the features not captured by (8) will be discussed later on.

The advantage of (8) is that it allows us to perform a rotation in the R-L space [17]

$$\begin{pmatrix} \psi_{n k s} \\ \phi_{n k s} \end{pmatrix} = \frac{1}{\sqrt{t_L^2 + t_R^2}} \begin{pmatrix} t_R & t_L \\ -t_L & t_R \end{pmatrix} \begin{pmatrix} c_{R n k s} \\ c_{L n k s} \end{pmatrix}, \quad (9)$$

after which the  $\phi$  field decouples from the dot:

$$H_T = \sqrt{t_L^2 + t_R^2} \sum_{n k s} \psi_{n k s}^\dagger d_{n s} + \text{H.c.} \quad (10)$$

The Hamiltonian of the system then acquires a form

$$\mathcal{H} = H_0(\phi) + H(\psi), \quad (11)$$

where  $H_0(\phi) = \sum_{n k s} \xi_{ks} \phi_{n k s}^\dagger \phi_{n k s}$  with  $\xi_{ks}$  given by Eq. (6) is the free-electron Hamiltonian of the  $\phi$ -particles, and

$$H(\psi) = H_0(\psi) + H_{dot} + H_T, \\ H_0(\psi) = \sum_{nks} \xi_{ks} \psi_{nks}^\dagger \psi_{nks} \quad (12)$$

describes the  $\psi$ -particles interacting with the dot via the tunneling Hamiltonian (10).

The physical quantity we are interested in is the linear conductance of the system  $G$ . The particle current operator is defined as

$$j = \frac{d}{dt} \frac{1}{2} (N_L - N_R), \quad N_\alpha = \sum_{nks} c_{\alpha nks}^\dagger c_{\alpha nks} \quad (13)$$

In order to take a full advantage of the decomposition (11), we need to express  $j$  via  $\psi$  and  $\phi$  of Eq. (9). When the resulting expression is substituted into the Kubo formula (see Appendix B for details of the calculation), it yields

$$G = \sum_{ns} g_0 \int d\varepsilon (-df/d\varepsilon) [-\pi\nu \text{Im} \mathcal{T}_{ns}(\varepsilon)]. \quad (14)$$

Here  $\mathcal{T}_{ns}$  are the diagonal elements of the  $\mathcal{T}$ -matrix for the Hamiltonian  $H(\psi)$ , defined in a usual fashion (see Appendix B),  $f$  is the Fermi function,  $\nu$  is the density of states in the leads, and

$$g_0 = \frac{e^2}{2\pi\hbar} \left( \frac{2t_L t_R}{t_L^2 + t_R^2} \right)^2. \quad (15)$$

In order to bring  $H(\psi)$  to the form convenient for further analysis, we explore the existence of a one-to-one correspondence between the low energy states of the dot (3) and the states of two fictitious 1/2-spins [11]:

$$\begin{aligned} |1, 1\rangle &\Longleftrightarrow |\uparrow_1 \uparrow_2\rangle, \\ |1, -1\rangle &\Longleftrightarrow |\downarrow_1 \downarrow_2\rangle, \\ |1, 0\rangle &\Longleftrightarrow \frac{1}{\sqrt{2}} (|\uparrow_1 \downarrow_2\rangle + |\downarrow_1 \uparrow_2\rangle), \\ |0, 0\rangle &\Longleftrightarrow \frac{1}{\sqrt{2}} (|\uparrow_1 \downarrow_2\rangle - |\downarrow_1 \uparrow_2\rangle), \end{aligned} \quad (16)$$

This correspondence allows one to represent any operator acting on the states (3) in terms of the spin-1/2 operators  $\mathbf{S}_{1,2}$ . By comparing directly matrix elements, one can check the validity of the following relations:

$$\mathcal{P} \sum_{ss'} d_{ns}^\dagger \frac{\boldsymbol{\sigma}_{ss'}}{2} d_{n's'} \mathcal{P} \equiv \frac{\delta_{n,n'}}{2} \mathbf{S}_+ + \frac{\delta_{n,-n'}}{2\sqrt{2}} (\mathbf{S}_- + 2in\mathbf{T}) \quad (17)$$

$$\mathcal{P} \sum_s d_{ns}^\dagger d_{n's} \mathcal{P} \equiv n \delta_{n,n'} [(\mathbf{S}_1 \cdot \mathbf{S}_2) - 1/4 + n] \quad (18)$$

Here  $\mathcal{P} = \sum_{S,S^z} |S, S^z\rangle \langle S, S^z|$  is a projector onto the low energy multiplet (3),  $\boldsymbol{\sigma} = (\sigma^x, \sigma^y, \sigma^z)$  are the Pauli matrices, and

$$\mathbf{S}_\pm = \mathbf{S}_1 \pm \mathbf{S}_2, \quad \mathbf{T} = \mathbf{S}_1 \times \mathbf{S}_2. \quad (19)$$

Eqs. (17)-(18) should be understood in a sense that the operators in the l.h.s. obey the same algebra as those in the r.h.s. The states (3) are the eigenstates of the operators  $\mathbf{S}_+$  and  $(\mathbf{S}_1 \cdot \mathbf{S}_2)$ , while  $\mathbf{S}_-$  and  $\mathbf{T}$  describe transitions between the singlet state and the components of the triplet. Some useful relations involving these operators are listed in Appendix A.

We can now simplify  $H(\psi)$  by integrating out the virtual transitions to the states with  $\mathcal{N} \pm 1$  electrons on the dot. This is done by means of the Schrieffer-Wolff transformation or, equivalently, of the second order of the Brillouin-Wigner perturbation theory. Using Eqs. (17)-(19), the result of this procedure is written in terms of the operators  $\mathbf{S}_{1,2}$  as [11]:

$$H = H_0(\psi) + K(\mathbf{S}_1 \cdot \mathbf{S}_2) - E_Z S_+^z + \sum_n H_n, \quad (20)$$

$$H_n = J(\mathbf{s}_{nn} \cdot \mathbf{S}_+) + V n \rho_{nn} (\mathbf{S}_1 \cdot \mathbf{S}_2) + \frac{I}{\sqrt{2}} [(\mathbf{s}_{-n,n} \cdot \mathbf{S}_-) + 2in(\mathbf{s}_{-n,n} \cdot \mathbf{T})]. \quad (21)$$

Here we introduced the particle and spin densities in the continuum:

$$\rho_{nn'} = \sum_{kk's} \psi_{nks}^\dagger \psi_{n'k's}, \quad \mathbf{s}_{nn'} = \sum_{kk'ss'} \psi_{nks}^\dagger \frac{\boldsymbol{\sigma}_{ss'}}{2} \psi_{n'k's'}. \quad (22)$$

The bare values of the coupling constants are

$$J = I = 2V = 2(t_L^2 + t_R^2)/E_C. \quad (23)$$

We did not include into (20)-(21) some terms, that are irrelevant for the low energy renormalization. The contribution of these terms to the conductance is featureless at the energy scale of the order of  $T_0$  (see the next section), where the Kondo resonance develops. The Schrieffer-Wolff transformation also produces a small correction to the energy gap  $K = E_{|1,0\rangle} - E_{|0,0\rangle}$  between the states  $|1,0\rangle$  and  $|0,0\rangle$ , so that  $K \neq K_0$ . However, this difference is not important, since it only affects the value of the control parameter at which the singlet-triplet transition occurs, but not the nature of the transition.

The effective Hamiltonian (20)-(21) can be simplified further by excluding the magnetic field acting on the electrons in the leads. Indeed, according to Eq. (14), the linear conductance is determined by the scattering properties of the  $\psi$ -particles in the vicinity of the Fermi level. It is therefore convenient to redefine the single particle energies in such a way that being measured from the corresponding Fermi levels they are independent of the spin direction  $\xi_{ks} \rightarrow \xi_k$ ,

$$H_0 = \sum_{nks} \xi_k \psi_{nks}^\dagger \psi_{nks}, \quad (24)$$

cf. Eq. (12). Most of the operators in the r.h.s. of (21) are invariant with respect to the redefinition of energies. The only correction that appears is

$$\sum_n J \langle s_{nn}^z \rangle_0 S_+^z = \nu J g_c \mu_B B S_+^z, \quad (25)$$

where  $\langle s_{nn}^z \rangle_0$  is ground state average of the spin density in the presence of the magnetic field (Note that  $J$  here is the *bare* value of the exchange amplitude). This correction can be readily absorbed into  $E_Z$  and can be cast in the form of a small (since  $\nu J \ll 1$ ) tunneling-induced correction to the  $g$ -factor  $g_d$  of the dot's electrons [see Eq. (2)], indistinguishable from other types of corrections [18]. Thus, not quite unexpectedly [19], the direct Zeeman coupling of the magnetic field to the electrons in the leads has little influence on the properties of the system.

There were several simplifying assumptions involved in the derivation of the effective Hamiltonian (20)-(21). Nevertheless, we believe it provides an adequate description of the low temperature physics in the vicinity of the singlet-triplet transition. The dot interacts via tunneling with four species, or channels, of conduction electrons. At the same time, the dot behaves like a composite two-spin impurity. Obviously, it takes only two channels to screen such an impurity. By analogy with the multi-channel Kondo model [21] one should expect that in the absence of special symmetry no more than two channels are coupled to the dot in the effective low energy Hamiltonian.

In the above derivation of the effective two-channel Hamiltonian we entirely ignored the multilevel structure of the dot and also adopted a simplified description of intradot Coulomb interaction. The presence of many energy levels in the dot is important at the energies above the single particle level spacing  $\delta$ , while the Kondo physics emerges at the energy scale well below  $\delta$ . These levels result merely in a renormalization of the parameters of the effective low energy Hamiltonian [20]. One only needs to consider this renormalization for deriving the relation between the parameters  $t_{ann'}$  of the low energy Hamiltonian (1), (6) and (7) to the “bare” constants of the model defined in a wide ( $\sim \epsilon_F$ ) band. On the other hand, using the effective low energy Hamiltonian, one can calculate, in principle, the observable quantities such as conductance  $G(T)$  and other susceptibilities of the system at low temperatures ( $T \ll \delta$ ), and establish the relations between them, which is our main goal.

The two-parameter ( $E_C, E_S$ ) description of the intradot Coulomb interaction, see Eq. (1), is justified as long as Random Matrix Theory (RMT) is applicable [16]. Small dots [7,8,14], containing only a few electrons, can not be described in the framework of RMT. Characterization of the interaction in such systems requires introduction of additional parameters. Respectively, the part of the effective Hamiltonian which describes the interaction

of the dot with itinerant electrons contains some additional [compared to Eq. (21)] constants, see Eq. (C1). Similar complications arise if the restriction (8) on the tunneling amplitudes is lifted, see Eq. (D2). Although the Hamiltonians (D2) and (C1) appear to be different and more cumbersome than Eq. (21), all three models turn out to be identical as far as one is interested in the low-temperature properties of the system. We will see in the next section that the three constants,  $J$ ,  $V$ , and  $I$  of the exchange Hamiltonian (21) grow in the course of renormalization. At a sufficiently advanced stage of the renormalization group procedure, these constants significantly exceed their starting values. It turns out, see Appendices C and D, that at such a stage the Hamiltonians (D2) and (C1) generate the same renormalization group (RG) flow as Eq. (21) does.

Note that the expression of the current operator (13) in terms of the fields  $\psi$  and  $\phi$  depends strongly on the manner in which  $\psi, \phi$  are composed from the original conduction electrons representing the left and the right leads. Therefore, lifting the restriction (8) results in modification of Eqs. (14), which express the DC conductance  $G$  through the properties of  $\psi$ -particles. In Section VII below we study in details the corresponding generalization of Eq. (14) onto the case of large Zeeman energy.

Also note that Eqs. (20)-(21) are valid only in the vicinity of the singlet-triplet transition. Far away from the transition, the system's properties can be much more complicated compared to the predictions based on (20)-(21). An example of such non-universal behavior is discussed in Appendix E.

The Hamiltonian (20)-(21) is still very complex and its exact treatment is very difficult, if possible at all. Fortunately, there exists a strong argument in favor of the Fermi-liquid nature of the ground state of (20)-(21). Indeed, formally, (20)-(21) resembles the effective Hamiltonian of the two-impurity Kondo model (2IKM), for which  $H_n$  is replaced by [22]

$$H_n^{2IKM} = J(\mathbf{s}_{nn} \cdot \mathbf{S}_+) + I(\mathbf{s}_{-n,n} \cdot \mathbf{S}_-) \quad (26)$$

and the parameter  $K$  characterizes the strength of the RKKY interaction. It is known [22] that 2IKM may undergo a phase transition at some special value of  $K$ . At this point, the system may exhibit non-Fermi liquid properties. However that this can happen [22] only if  $H$  is invariant with respect to the particle-hole transformation

$$\psi_{nks} \rightarrow s\psi_{n,-k,-s}^\dagger.$$

The two extra terms in (21) as compared to (26) violate this invariance. Therefore, the symmetry that warrants the existence of the non-Fermi liquid state is absent in our problem. The logarithmic grow of the two extra terms in (21) at low energies [11] precludes the possibility that the RG flow passes anywhere near the 2IKM non-Fermi liquid fixed point.

#### IV. SCALING ANALYSIS

To gain an insight into the low-energy properties of our model, we apply the “poor man’s” scaling technique [23]. The procedure consists of a successive integration out of the high-energy degrees of freedom and yields a set of scaling equations [11]

$$\begin{aligned} dJ/d\mathcal{L} &= \nu(J^2 + I^2), \\ dI/d\mathcal{L} &= 2\nu I(J + V), \\ dV/d\mathcal{L} &= 2\nu I^2 \end{aligned} \quad (27)$$

with the initial conditions (23). Here  $\mathcal{L} = \ln(\delta/D)$ , and  $\nu$  is the density of states in the leads; the initial value of the high energy cutoff  $D$  is  $D = \delta$ , see the discussion after Eq. (23). The scaling procedure also generates corrections to  $K$ . In the following we absorb these corrections in the re-defined value of  $K$ . Equations (27) are valid in the perturbative regime and as long as

$$D \gg |K|, E_Z, T.$$

At certain value of the scale,  $\mathcal{L} = \mathcal{L}_0$ , the inverse coupling constants simultaneously reach zero:

$$1/J(\mathcal{L}_0) = 1/I(\mathcal{L}_0) = 1/V(\mathcal{L}_0) = 0.$$

This can be used to define a characteristic energy scale of the problem  $T_0$  through the equation

$$\ln(\delta/T_0) = \mathcal{L}_0.$$

The value of  $T_0$  is obviously non-universal. It is convenient to parametrize  $T_0$  by a value of constant  $c$  in the expression resembling the usual definition of Kondo temperature:

$$T_0 = \delta \exp[-c/\nu J]; \quad (28)$$

here  $J = J(\mathcal{L} = 0)$  is given by Eq. (23). For the special choice (8) of the tunneling amplitudes it was found numerically [11] that  $c = 0.36$ . It is instructive to compare  $T_0$  with the Kondo temperature  $T_K^{\text{triplet}}$ , corresponding to  $K = -\delta$  at the triplet side of the singlet-triplet transition (see the next Section),

$$T_K^{\text{triplet}} = \delta \exp[-1/\nu J], \quad (29)$$

and with the Kondo temperature  $T_K^{\text{odd}}$  in the adjacent Coulomb blockade valleys with  $N = \text{odd}$ . In the latter case, only one of the two orbitals  $n = \pm 1$  in the dot is involved in the corresponding effective Hamiltonian, which takes the form of a single-channel  $S = 1/2$  Kondo model. The corresponding exchange amplitude is  $J_{\text{odd}} = 4(t_L^2 + t_R^2)/E_C = 2J$ , which yields

$$T_K^{\text{odd}} = \delta \exp[-1/2\nu J]. \quad (30)$$

[note that (29) and (30) are also valid only for the model (8)]. In the limit  $\nu J \rightarrow 0$  Eqs. (28)-(30) imply that

$$T_0 \gg T_K^{\text{odd}} \gg T_K^{\text{triplet}}.$$

This inequality explains why the Kondo effect at the singlet-triplet transition point in the  $N = \text{even}$  valley appears more pronounced than that in the  $N = \text{odd}$  valleys [7], and why the experiments with vertical quantum dots failed to detect the Kondo effect away from the transition when the dot definitely was in the triplet state [7].

The solution of the RG equations (27) can be expanded near  $\mathcal{L} = \mathcal{L}_0$ . To the first order in  $\mathcal{L}_0 - \mathcal{L} = \ln D/T_0$ , we obtain

$$\frac{1}{\nu J} = \frac{\sqrt{\lambda}}{\nu I} = \frac{\lambda - 1}{2\nu V} = (\lambda + 1) \ln(D/T_0), \quad (31)$$

where

$$\lambda = 2 + \sqrt{5} \approx 4.2. \quad (32)$$

It should be emphasized that the constant  $\lambda$  is determined by the properties of the solutions of (27) at large  $\mathcal{L}$  and is universal in the sense that its value does not depend on the bare values of the coupling constants.

The solution (31) can be used to calculate the differential conductance at high temperature  $T \gg |K|, T_0$ . In this regime, the coupling constants are still small, and the conductance can be calculated perturbatively from the Hamiltonian (20)-(21) with renormalized parameters and formula (14). This results in

$$G/G_0 = \frac{A}{[\ln(T/T_0)]^2}, \quad (33)$$

where  $G_0 = 4g_0$  and

$$A = (3\pi^2/8) (\lambda + 1)^{-2} \left[ 1 + \lambda + (\lambda - 1)^2/8 \right] \approx 0.9$$

is a numerical constant. At low temperature, the RG flow (27) terminates at either  $D \sim |K|$  (which corresponds to the relatively strong orbital effect of the magnetic field), or at  $D \sim E_Z$  (weak orbital effect). We consider these two cases separately.

#### V. SINGLET-TRIPLET TRANSITION

In this section, we assume that the Zeeman energy is negligibly small compared to all other energy scales. At high temperature  $T \gtrsim |K|$ , the conductance is given by Eq. (33). At low temperature  $T \lesssim |K|$  and away from the singlet-triplet degeneracy point,  $|K| \gtrsim T_0$ , the RG flow yielding Eq. (33) terminates at energy  $D \sim |K|$ . On the *triplet* side of the transition,

$$K \ll -T_0,$$

the two spins  $\mathbf{S}_{1,2}$  are locked together into a triplet. The system is therefore described by the effective two-channel Kondo model with  $S = 1$  impurity, obtained from Eqs. (20)-(21) by projecting out the singlet state and dropping the no longer relevant potential scattering term:

$$H_{\text{triplet}} = H_0 + J \sum_n (\mathbf{s}_{nn} \cdot \mathbf{S}). \quad (34)$$

Here  $J$  is given by the solution  $J(\mathcal{L})$  of Eq. (27), taken at  $\mathcal{L} = \mathcal{L}^* = \ln(\delta/|K|)$ , which corresponds to  $D = |K|$ . With further decrease of  $D$  the renormalization of the exchange amplitude  $J$  is governed by the standard RG equation [23]

$$dJ/d\mathcal{L} = \nu J^2, \quad \mathcal{L} > \mathcal{L}^*. \quad (35)$$

The solution of Eq. (35),

$$1/\nu J(\mathcal{L}) - 1/\nu J(\mathcal{L}^*) = \mathcal{L} - \mathcal{L}^*,$$

can be also written as  $1/\nu J = \ln(D/T_K)$  in terms of the running bandwidth  $D$  and the Kondo temperature

$$T_K(K) = |K| \exp[-1/\nu J(\mathcal{L}^*)]. \quad (36)$$

Substituting here the asymptote of  $J(\mathcal{L}^*)$  from Eq. (31) we obtain

$$\frac{T_K}{T_0} = \left( \frac{T_0}{|K|} \right)^\lambda. \quad (37)$$

This result is universal and is valid in the vicinity of the transition point. To clarify what does the "vicinity" mean, we again rely on the model (8), for which Eqs. (27) are valid for all  $|K| \lesssim \delta$ . Expansion of the solution of Eqs. (27) near the weak coupling fixed point  $\mathcal{L} = 0$  and the substitution of  $J(\mathcal{L}^*)$  into (36) results in the large- $|K|$  asymptote of  $T_K(K)$ :

$$\frac{T_K(K)}{T_K^{\text{triplet}}} = \frac{\delta}{|K|}, \quad (38)$$

where  $T_K^{\text{triplet}}$  is given by Eq. (29). Comparison of (37) and (38) shows that the two asymptotes match at

$$|K|/T_0 = (\delta/T_0)^\mu, \quad \mu = \frac{1/c - 2}{\lambda - 1} \approx 0.24,$$

which gives the upper limit of the validity of Eq. (37):  $|K|/T_0 \ll (\delta/T_0)^\mu$ . From Eqs. (37),(38) follows that the larger is  $|K|$  the smaller  $T_K$  is. In fact, the universal part  $T_K(K)$ , Eq. (29), suffices to describe a fall of  $T_K$  by an order of magnitude for realistic values of the parameters for a vertical quantum dot device [10].

For a given  $|K| \gtrsim T, T_0$  the linear conductance can be cast into the scaling form,

$$G/G_0 = F(T/T_K) \quad (39)$$

where  $F(x)$  is a smooth function that interpolates between  $F(x \gg 1) = (\pi^2/2)(\ln x)^{-2}$  and  $F(0) = 1$ . It coincides with the scaled resistivity

$$F(T/T_K) = \rho(T/T_K)/\rho(0)$$

for the symmetric two channel  $S = 1$  Kondo model. The conductance at  $T = 0$  (the unitary limit value) is  $G_0 = 4g_0$ , see Eq. (15). Equation (39) remains valid not too far away from the transition point, where the universal description (20)-(21) is applicable. At large  $|K|$  the conductance exhibit additional features (an example is discussed in Appendix E). However, smallness of  $T_K$  renders these features difficult to observe.

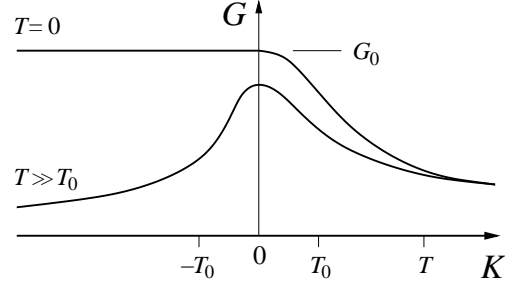


FIG. 2. Linear conductance near a singlet-triplet transition. At high temperature  $G$  exhibits a peak near the transition point. At low temperature  $G$  reaches the unitary limit at the triplet side of the transition, and decreases monotonously at the singlet side. The two asymptotes merge at  $K \gg T, T_0$ .

On the *singlet* side of the transition,

$$K \gg T_0,$$

the scaling terminates at  $D \sim K$ , and the low-energy effective Hamiltonian is

$$H_{\text{singlet}} = H_0 - \frac{3}{4}V \sum_n n \rho_{nn},$$

where  $V$  is the renormalized scattering amplitude  $V(\mathcal{L})$  taken at  $\mathcal{L} = \mathcal{L}^* = \ln(\delta/|K|)$ . The temperature dependence of the conductance saturates at  $T \lesssim K$ , reaching the value

$$G/G_0 = \frac{B}{[\ln(K/T_0)]^2}, \quad B = \left( \frac{3\pi}{8} \frac{\lambda - 1}{\lambda + 1} \right)^2 \approx 0.5. \quad (40)$$

This result is universal in the vicinity of the transition.

At  $T = 0$  Eqs. (39) and (40) predict different dependence on the parameter  $K$  which is used for tuning through the transition. At positive  $K$ , conductance decreases with the increase of  $K$ , while at  $K \ll -T_0$  conductance  $G$  is independent of  $K$ , see Fig. 2. While the conductance  $G$  is a monotonous function of  $K$  at  $T = 0$ , it develops a *peak* at the singlet-triplet transition point  $K = 0$  at high temperature  $T \gg T_0$ .

## VI. TRANSITION DRIVEN BY ZEEMAN SPLITTING

If the Zeeman energy is large, the RG flow (27) terminates at  $D \sim E_Z$ . The effective Hamiltonian, valid at the energies  $D \lesssim E_Z$  is obtained by projecting (20)-(21) onto the states  $|1, 1\rangle$  and  $|0, 0\rangle$ . These states differ by a flip of a spin of a single electron (see Fig. 3), and are the counterparts of the spin-up and spin-down states of  $S = 1/2$  impurity in the conventional Kondo problem. It is therefore convenient to switch to the notations [15]

$$|1, 1\rangle = |\uparrow\rangle, \quad |0, 0\rangle = |\downarrow\rangle, \quad (41)$$

and to describe the transitions between the two states in terms of the (pseudo)spin operator

$$\tilde{\mathbf{S}} = \frac{1}{2} \sum_{ss'} |s\rangle \boldsymbol{\sigma}_{ss'} \langle s'|,$$

built from the states (41).

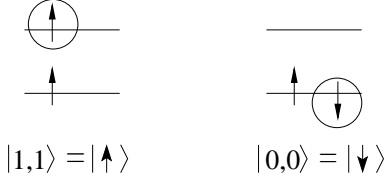


FIG. 3. The ground state doublet in case of a large Zeeman splitting. The states  $|1, 1\rangle$  and  $|0, 0\rangle$  differ by flipping a spin of a single electron (marked by circles).

Among the various operators in (20)-(21) that act on the states of the dot only the following have non-zero matrix elements between the states (41):

$$\begin{aligned} \mathcal{P}' S_+^z \mathcal{P}' &= \tilde{S}^z + 1/2, \quad \mathcal{P}' (\mathbf{S}_1 \cdot \mathbf{S}_2) \mathcal{P}' = \tilde{S}^z - 1/4, \\ \mathcal{P}' S_-^z \mathcal{P}' &= -\sqrt{2} \tilde{S}^\pm, \quad \mathcal{P}' T^\pm \mathcal{P}' = \pm \frac{i}{\sqrt{2}} \tilde{S}^\pm, \end{aligned}$$

where  $\mathcal{P}' = \sum_s |s\rangle \langle s|$ . Using these relations, we obtain from (20)-(21)

$$\begin{aligned} H &= \sum_{nks} \xi_k \psi_{nks}^\dagger \psi_{nks} - \Delta \tilde{S}^z \\ &+ \sum_n \left[ J s_{nn}^z (\tilde{S}^z + 1/2) + V n \rho_{nn} (\tilde{S}^z - 1/4) \right] \\ &- I (s_{1,-1}^+ \tilde{S}^- + \text{H.c.}), \end{aligned} \quad (42)$$

where  $\Delta = E_Z - K$ , see Eq. (5). It is now convenient to transform (42) to a form which is diagonal in the orbital indexes  $n$ . This is achieved by relabeling the fields according to

$$\begin{aligned} \psi_{+1,k,\uparrow} &= a_{k,\uparrow}, \quad \psi_{-1,k,\downarrow} = -a_{k,\downarrow}, \\ \psi_{-1,k,\uparrow} &= b_{k,\uparrow}, \quad \psi_{+1,k,\downarrow} = -b_{k,\downarrow}, \end{aligned} \quad (43)$$

which yields

$$\begin{aligned} H &= H_0 - \Delta \tilde{S}^z \\ &+ V_a s_a^z + J_z s_a^z \tilde{S}^z + \frac{1}{2} J_\perp (s_a^+ \tilde{S}^- + s_a^- \tilde{S}^+) \\ &+ V_b s_b^z + J'_z s_b^z \tilde{S}^z, \end{aligned} \quad (44)$$

where  $H_0$  is a free-particle Hamiltonian for  $a, b$  electrons, and  $\mathbf{s}_a = \sum_{kk'ss'} a_{ks}^\dagger (\boldsymbol{\sigma}_{ss'}/2) a_{k's'}$  is the spin density for  $a$ -electrons (with a similar definition for  $\mathbf{s}_b$ ). The coupling constants in (44),

$$\begin{aligned} V_a &= (J - V)/2, \quad J_z = J + 2V, \quad J_\perp = 2I, \\ V_b &= (J + V)/2, \quad J'_z = J - 2V \end{aligned} \quad (45)$$

are expressed through the solutions of the RG equations (27) taken at  $\mathcal{L} = \mathcal{L}^* = \ln(\delta/E_Z)$ .

Eq. (52) contains unusual terms  $V_i s_i^z$ , which have a meaning of a magnetic field acting *locally* on the conduction electrons at the impurity site. The appearance of these terms is a price of the finiteness of the magnetic field, which breaks spin-rotational invariance. Fortunately, these terms do not change significantly properties of the model. Their main effect is to produce a small correction to  $\Delta$ , through creating a non-zero expectation value  $\langle s_i^z \rangle$ . This correction is not important, since it merely shifts the degeneracy point. In addition,  $V_i s_i^z$  lead to insignificant corrections to the densities of states [15]. In the following, we will discard these terms.

The scaling equations for the coupling constants in (44) take the standard form [23]

$$dJ_z/d\mathcal{L} = \nu J_\perp^2, \quad dJ_\perp/d\mathcal{L} = \nu J_z J_\perp, \quad \mathcal{L} > \mathcal{L}^*; \quad (46)$$

$J'_z$  is not renormalized in this order of perturbation theory, but acquires a negative correction in the next order:  $dJ'_z/d\mathcal{L} = -\frac{1}{2} \nu^2 J_\perp^2 J'_z$ . In addition,  $J'_z$  initially is smaller than  $J_z$  (for  $E_Z = \delta$ , for example,  $J'_z$  simply vanishes). Therefore the  $b$ -dependent part of (44) can be ignored, and the resulting effective Hamiltonian is that of a single-channel  $S = 1/2$  anisotropic Kondo model [15].

The Kondo temperature  $T_K$  depends on  $E_Z$ . For the model (8), as follows from Eqs. (23) and (45), the exchange at  $E_Z = \delta$  is isotropic:  $J_z = J_\perp = 2J$  (where  $J$  is given by (23)). Therefore the Kondo temperature  $T_K^{\text{Zeeman}}$  corresponding to  $E_Z = \delta$  satisfies

$$T_K^{\text{Zeeman}} = T_K^{\text{odd}},$$

see Eq. (30). At lower  $E_Z$  the Kondo temperature becomes larger. Interestingly, the isotropy of the exchange in (44) is preserved in the regime when Eqs. (27) can be linearized near  $\mathcal{L} = 0$ . The corresponding asymptote of  $T_K(E_Z)$  is

$$\frac{T_K(E_Z)}{T_K^{\text{Zeeman}}} = \left( \frac{\delta}{E_Z} \right)^{1/2} \quad (47)$$



When  $E_Z$  approaches  $T_0$  one can use Eqs. (31) to calculate initial conditions for (46). From (31) and (45) follows that the difference between  $J_z$  and  $J_\perp$  in this regime is very small:  $J_z/J_\perp = \sqrt{\lambda}/2 \approx 1.02$ . Therefore, the anisotropy of the exchange can be neglected in the universal regime as well, and we obtain

$$\frac{T_K}{T_0} = \left( \frac{T_0}{E_Z} \right)^{1/\lambda}. \quad (48)$$

The asymptotes (47) and (48) match at

$$E_Z/T_0 = (\delta/T_0)^{\mu'}, \quad \mu' = \frac{3-1/c}{1-2/\lambda} \approx 0.42,$$

which separates their regions of applicability. The dependence of  $T_K$  on  $E_Z$  appears to be much weaker than the dependence of  $T_K$  on  $K$  in the previous section, and practically saturates in the regime (48).

The linear conductance is given by [cf. Eq. (14)]

$$G = \sum_s g_0 \int d\varepsilon (-df/d\varepsilon) [-\pi\nu \text{Im} \mathcal{T}_s^a(\varepsilon)], \quad (49)$$

where  $\mathcal{T}_s^a$  is the  $\mathcal{T}$ -matrix for the  $a$ -particles with spin  $s$ ;  $\mathcal{T}_s^a$  does not depend on  $s$  if the term  $V_a s_a^z$  in (44) is neglected. The distance to the degeneracy point  $\Delta$  in Eq. (44) plays the part of the Zeeman splitting of the impurity spin in the conventional Kondo effect. At  $\Delta = 0$  the Kondo resonance develops: Regardless the initial anisotropy of the exchange constants in Eq. (52), the conductance in the universal regime (when  $T$  approaches the Kondo temperature  $T_K$  or lower) is given by

$$G = G_0 f(T/T_K), \quad (50)$$

where  $f(x)$  is a smooth function interpolating between  $f(0) = 1$  and  $f(x \gg 1) = (3\pi^2/16)(\ln x)^{-2}$ . Function  $f(T/T_K)$  coincides with the scaled resistivity for the single channel  $S = 1/2$  Kondo model and its detailed shape is known [25]. Note that in (50) the zero-temperature conductance  $G_0 = 2g_0$  is by a factor of 2 smaller than that in Eqs. (33),(39),(40).

At finite  $\Delta \gg T_K$ , the scaling trajectory (46) terminates at  $D \sim \Delta$ . Below this energy scale the spin-flip scattering processes are suppressed. As a result, at  $T \ll \Delta$  the linear conductance is given by

$$G = G_0 \frac{\pi^2/16}{[\ln(\Delta/T_K)]^2} \quad (51)$$

and is independent of temperature.

## VII. SPIN FILTERING AND ASYMMETRY OF THE NON-LINEAR CONDUCTANCE CAUSED BY ZEEMAN SPLITTING

The low-temperature properties of the system exhibiting the Zeeman-splitting-driven Kondo effect can be de-

scribed by a single-channel anisotropic Kondo Hamiltonian

$$\mathcal{H} = H_0(\phi) + H_0(\psi) - \Delta \tilde{S}^z + U s^z + J_z s^z \tilde{S}^z + \frac{J_\perp}{2} (s^+ \tilde{S}^- + s^- \tilde{S}^+), \quad (52)$$

where  $\mathbf{s} = \sum_{kk'ss'} \psi_{ks}^\dagger (\boldsymbol{\sigma}_{ss'}/2) \psi_{k's'}$ . This description is valid regardless the assumption (8). The operators  $\psi_{ks}$  are certain linear combinations of the conduction electron operators from the left and right leads. When the restriction (8) is lifted, the coefficients of such linear relation are  $s$ -dependent [15]:

$$\begin{pmatrix} \psi_{ks} \\ \phi_{ks} \end{pmatrix} = \begin{pmatrix} \cos \vartheta_s & \sin \vartheta_s \\ -\sin \vartheta_s & \cos \vartheta_s \end{pmatrix} \begin{pmatrix} c_{Rks} \\ c_{Lks} \end{pmatrix}. \quad (53)$$

Perhaps, the simplest possible generalization of (8) yielding  $\vartheta_{+1} \neq \vartheta_{-1}$  in (53) is  $t_{\alpha nn'} = t_{\alpha n} \delta_{nn'}$  [see Appendix E, Eq. (E1)], in which case  $\tan \vartheta_s = t_{Ls}/t_{Rs}$ .

The  $s$ -dependence of the coefficients in (53) may lead to interesting effects. We consider the linear regime first. It is convenient to split the current operator (13) into two parts,

$$j = j_0 + \delta j,$$

which are respectively bi-linear and quadratic in the operators  $\psi$  and  $\phi$ . Using Eq. (53) we obtain

$$j_0 = \frac{d}{dt} \frac{1}{2} \sum_{ks} \sin(2\vartheta_s) (\psi_{ks}^\dagger \phi_{ks} + \phi_{ks}^\dagger \psi_{ks}) \quad (54)$$

$$\delta j = \frac{d}{dt} \frac{\eta}{2} \sum_s s \psi_{ks}^\dagger \psi_{ks}, \quad \eta = \sum_s s \sin^2 \vartheta_s. \quad (55)$$

The operator  $\delta j$  makes no contribution to the DC conductance. Indeed, since  $\frac{1}{2} \sum_s s \psi_{ks}^\dagger \psi_{ks} + \tilde{S}^z$  commutes with  $\mathcal{H}$ , Eq. (55) can be re-written as

$$\delta j = -\eta \frac{d}{dt} \tilde{S}^z. \quad (56)$$

Being averaged over time,  $\delta j$  yields 0:

$$\begin{aligned} \overline{\langle \delta j \rangle} &= \lim_{t_0 \rightarrow \infty} \frac{1}{2t_0} \int_{-t_0}^{t_0} dt \langle \delta j(t) \rangle \\ &= \lim_{t_0 \rightarrow \infty} \frac{\eta}{2t_0} \langle \tilde{S}^z(-t_0) - \tilde{S}^z(t_0) \rangle = 0 \end{aligned}$$

because operator  $\tilde{S}^z$  is bounded,  $-1/2 \leq \langle \tilde{S}^z(t) \rangle \leq 1/2$ . Thus, the contribution  $\delta G$  from  $\delta j$  to the DC conductance *vanishes identically*.

The contribution from  $j_0$  is evaluated in the same way as in Appendix B with the result

$$G = \sum_s g_0^s \int d\varepsilon (-df/d\varepsilon) [-\pi\nu \text{Im}\mathcal{T}_s(\varepsilon)], \quad (57)$$

where

$$g_0^s = \frac{e^2}{2\pi\hbar} \sin^2(2\vartheta_s)$$

and  $\mathcal{T}_s$  is  $\mathcal{T}$ -matrix for  $\psi$ -particles with spin  $s$ . Equation (49) is identical to Eq. (57), except for  $s$ -dependence of  $g_0^s$ . Therefore, the conductance at sufficiently low temperature is again given by Eqs. (50) and (51) with  $G_0 = \sum_s g_0^s$ .

At  $T = 0$  the electrons scatter from the dot elastically [24], that is, without flip of their spin. In this regime the inequality  $g_0^{+1} \neq g_0^{-1}$  means that the probability of transmission through the dot depends on the direction of the spin of an incoming electron. In other words, the system acts as a *spin filter* [15].

The main effect for the *non-linear* differential conductance  $dI/dV_{DC}$  consists in the violation of symmetry with respect to the bias sign. To see this, it is sufficient to calculate the conductance in the leading (second) order of the perturbation theory in  $J_\perp$ . In this order, tunneling of an electron through the dot is accompanied by the transition of the dot between the states  $|\uparrow\rangle$  and  $|\downarrow\rangle$ , see Eq. (41). The difference of the corresponding energies,  $E_{|\uparrow\rangle} - E_{|\downarrow\rangle}$ , depends on the average value of the operator  $s^z$  through the term  $J_z s^z \tilde{S}^z$  in the Hamiltonian (52). This average is not zero due to a *finite* DC voltage bias  $V_{DC}$ , which is described by an addition of a term

$$H_V = \frac{eV_{DC}}{2}(N_L - N_R) \quad (58)$$

to the Hamiltonian (52). Using (53) and (58) we obtain

$$\begin{aligned} \langle s^z \rangle &= \sum_{ks} \frac{s}{2} \left[ \langle c_{Rks}^\dagger c_{Rks} \rangle \cos^2 \vartheta_s + \langle c_{Lks}^\dagger c_{Lks} \rangle \sin^2 \vartheta_s \right] \\ &= -\frac{\eta}{2} \nu eV_{DC}, \end{aligned}$$

where  $\eta$  is given by (55). Therefore, the energy difference between the states (41) acquires a bias-dependent correction:

$$\begin{aligned} E_{|\downarrow\rangle} - E_{|\uparrow\rangle} &= \Delta + \delta\Delta, \\ \delta\Delta &= J_z \langle s^z \rangle = \chi eV_{DC}, \quad \chi = \eta\nu J_z/2. \end{aligned} \quad (59)$$

This correction is similar to that caused by the magnetic field applied to the leads, see Eq. (25). But there is an important difference:  $\delta\Delta$  in Eq. (59) is due to *non-equilibrium*. Obviously, the contribution to the non-linear conductance we discuss is suppressed if  $|eV_{DC}| < E_{|\uparrow\rangle} - E_{|\downarrow\rangle}$ . Using Eq. (59) we find for the interval of suppression

$$-\frac{\Delta}{1+\chi} < eV_{DC} < \frac{\Delta}{1-\chi}. \quad (60)$$

Similar to the conventional Kondo problem [4] higher-order calculation yields the differential conductance which peaks at the ends of the interval (60). Therefore the position of peaks is not symmetric with respect to the change of the bias polarity  $V_{DC} \rightarrow -V_{DC}$ , see Fig. 4.

The feasibility of an experimental observation of this effect obviously depends on the value of the parameter  $\eta$ . The largest possible value  $|\eta| = 1$  is reached in a strongly asymmetric setup. An example of such setup consists of level  $n = +1$ , see Fig. 3, coupled only to the left lead, while the level  $n = -1$  is coupled only to the right lead. Such a control over the tunneling amplitudes to the individual energy levels in the dot is very difficult to achieve with a single-dot device. But one can instead think of a system of two very small quantum dots connected *in series* [26]. If the gate voltages are tuned properly, the double-dot system is equivalent to a single dot with  $N = \text{even}$ . In particular, the situation is possible when the wave functions of the upper and lower levels in Fig. 3 are localized mostly in the left and in the right dots respectively. The degree of the “localization” and, therefore, the value of the parameter  $\eta$  is controlled by the strength of the tunneling coupling between the dots.

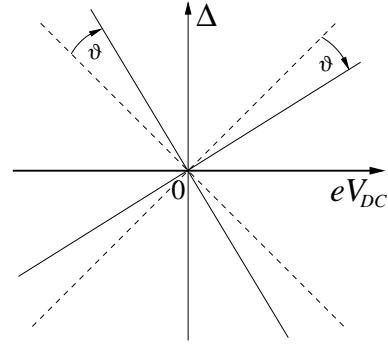


FIG. 4. Position of the peaks of differential conductance at  $(eV_{DC}, \Delta)$ -plane. The dashed lines correspond to  $eV_{DC} = \pm\Delta$ . The angle  $\vartheta \approx \chi/2 = \eta\nu J_z/4 \ll 1$  can be either positive or negative, depending on the sign of the non-universal parameter  $\eta$ .

Note that similar non-linear effects occur also in the case of a small Zeeman splitting,  $E_Z \ll T_0$ , considered in Section V. At a finite temperature and when the system is tuned to the singlet-triplet transition point, the differential conductance exhibits a peak at zero bias. The peak is split in two when the magnetic field is tuned away from the transition. The location of the split peaks is given by the energy balance condition for activation of the interorbital scattering processes:  $|eV_{DC}| = K + \delta K$ . Here  $\delta K \propto eV_{DC}$  is a non-universal correction analogous to  $\delta\Delta$  in (59), which appears due to a non-zero average of the operator  $\sum_n n \rho_{nn}$  in Eq. (21) in the presence of a finite bias.

## CONCLUSION

In this paper we studied the transport through a quantum dot tuned to the singlet-triplet transition point. Such a transition in the ground state of an isolated dot can be reached by applying a magnetic field to it. The low temperature properties of a quantum dot attached to conducting leads can be described by a version of a two-impurity Kondo model. Depending on the value of Zeeman energy, two distinct physical situations are realized.

If Zeeman energy is small, the zero-temperature linear conductance reaches the quantum limit at the triplet side of the transition. At finite temperature, however, the conductance reaches a maximum at the transition point. This happens due to the extra degeneracy of the ground state multiplet of the dot at this point, which causes an increase of the characteristic temperature below which the conductance is approaching the unitary limit.

If Zeeman energy is large, the ground state of the dot is degenerate only at the transition point. In this limit the model can be further reduced to the single-channel anisotropic Kondo Hamiltonian. The conductance exhibits a peak at the point of the transition at arbitrary low temperature.

The two limits of the theory are in a good agreement with the results of recent experiments with vertical quantum dots and carbon nanotubes.

## ACKNOWLEDGMENTS

This work was supported by NSF under Grants DMR-9812340 and DMR-9731756. We benefited from discussions with D. Cobden, M. Eto, K. Kikoin, L. Kouwenhoven, A. Ludwig, A. Luther, K. Matveev, Yu. Nazarov, S. Tarucha, A. Tsvetlik, M. Voloshin, J. Weis, and A. Zvyagin.

## APPENDIX A: SOME PROPERTIES OF THE OPERATORS $\mathbf{S}_\pm$ AND $\mathbf{T}$

Using  $[S_i^\alpha, S_j^\beta] = \delta_{ij} \sum_\gamma \epsilon_{\alpha\beta\gamma} S_i^\gamma$ , it is straightforward to show that the operators  $\mathbf{S}_\pm = \mathbf{S}_1 \pm \mathbf{S}_2$  and  $\mathbf{T} = \mathbf{S}_1 \times \mathbf{S}_2$  obey the commutation relations

$$\begin{aligned} (\mathbf{S}_- \cdot \mathbf{T}) - (\mathbf{T} \cdot \mathbf{S}_-) &= 4i(\mathbf{S}_1 \cdot \mathbf{S}_2), \\ [\mathbf{S}_-, (\mathbf{S}_1 \cdot \mathbf{S}_2)] &= -2i\mathbf{T}, \\ [\mathbf{T}, (\mathbf{S}_1 \cdot \mathbf{S}_2)] &= \frac{i}{2}\mathbf{S}_-. \end{aligned}$$

Using these relations one can check that  $\mathbf{S}_-$  and  $\mathbf{T}$  are related by means of the unitary transformation

$$2\mathbf{T} = e^{-i\frac{\pi}{2}(\mathbf{S}_1 \cdot \mathbf{S}_2)} \mathbf{S}_- e^{i\frac{\pi}{2}(\mathbf{S}_1 \cdot \mathbf{S}_2)}.$$

Since  $(\mathbf{S}_1 \cdot \mathbf{S}_2)$  commutes with  $\mathbf{S}_+$ , application of this transformation to the identity

$$[S_\pm^\alpha, S_\mp^\beta] = \sum_\gamma i\epsilon_{\alpha\beta\gamma} S_\mp^\gamma,$$

gives at once

$$[S_+^\alpha, T^\beta] = \sum_\gamma i\epsilon_{\alpha\beta\gamma} T^\gamma, \quad [T^\alpha, T^\beta] = \frac{1}{4} \sum_\gamma i\epsilon_{\alpha\beta\gamma} S_+^k.$$

## APPENDIX B: DERIVATION OF EQ. (14)

Using Eq. (9), the particle current operator  $j$  is written as

$$j = \frac{t_L t_R}{t_L^2 + t_R^2} \sum_{nks} \frac{d}{dt} A_{nks} + \text{H.c.}, \quad A_{nks} = \psi_{nks}^\dagger \phi_{nks}$$

Substitution into the Kubo formula

$$G = \lim_{\omega \rightarrow 0} \frac{e^2}{\hbar} \frac{1}{\omega} \int_0^\infty dt e^{i\omega t} \langle [j(t), j(0)] \rangle, \quad (\text{B1})$$

and integration by parts yield

$$G = - \lim_{\omega \rightarrow 0} g_0 \pi \omega \sum_{nks} \text{Im} \Pi_{nks}(\omega), \quad (\text{B2})$$

where  $g_0$  is given by Eq. (15) and  $\Pi_{nks}(\omega) = \int dt e^{i\omega t} \Pi_{nks}(t)$  is the Fourier-transform of the retarded correlation function

$$\Pi_{nks}(t) = -i\theta(t) \left\langle [A_{nks}(t), A_{nks}^\dagger(0)] \right\rangle$$

One can express  $\Pi_{nks}(\omega)$  via the retarded Green functions of the  $\psi$  and  $\phi$  particles as

$$\begin{aligned} \text{Im} \Pi_{nks}(\omega) &= \frac{1}{\pi} \int d\epsilon [f(\epsilon + \omega) - f(\epsilon)] \\ &\quad \times \text{Im} \mathcal{G}_{nks}^0(\epsilon) \text{Im} \mathcal{G}_{nks}(\epsilon + \omega), \end{aligned} \quad (\text{B3})$$

where  $f(\epsilon)$  is the Fermi function, and  $\mathcal{G}_{nks}(\epsilon)$  is the Fourier-transform of

$$\mathcal{G}_{nks}(t) = -i\theta(t) \langle \{\psi_{nks}(t), \psi_{nks}^\dagger(0)\} \rangle.$$

In writing of Eq. (B3) we took into account that the Green function of the  $\phi$ -particles coincides with the unperturbed (without interactions) value of  $\mathcal{G}_{nks}$ ,

$$\mathcal{G}_{nks}^0(\epsilon) = (\epsilon - \xi_{ks} + i0)^{-1}.$$

Therefore  $\text{Im} \mathcal{G}_{nks}(\epsilon) = -\pi \delta(\epsilon - \xi_{ks})$ , which removes the integral over  $\epsilon$  in (B3). It is convenient to represent  $\mathcal{G}_{nks}$  in the form

$$\mathcal{G}_{nks}(\epsilon) = \mathcal{G}_{nks}^0(\epsilon) + \mathcal{G}_{nks}^0(\epsilon) \mathcal{T}_{nks}(\epsilon) \mathcal{G}_{nks}^0(\epsilon), \quad (\text{B4})$$

where  $\mathcal{T}_{nks}(\epsilon)$  is a diagonal element of the  $\mathcal{T}$ -matrix. Since the interaction in  $H(\psi)$  is local,  $\mathcal{T}_{nks}(\epsilon)$  is in fact independent of  $k$ :  $\mathcal{T}_{nks} = \mathcal{T}_{ns}$ . Obviously, for  $\epsilon = \xi_{ks} + \omega$  the second term in the r.h.s. of (B4) diverges as  $\omega^{-2}$  at small  $\omega$ . Combination of Eq. (B4) with Eqs. (B2) and (B3), and replacement of the sum over  $k$  in Eq. (B2) by an integral then yield Eq. (14).

### APPENDIX C: THE EFFECTIVE EXCHANGE HAMILTONIAN FOR THE GENERAL FORM OF INTRADOT INTERACTIONS

Two electrons occupying two single particle energy levels can form three linearly independent singlet states:

$$\begin{aligned} |0,0\rangle_{-1} &= d_{-1\uparrow}^\dagger d_{-1\downarrow}^\dagger |0\rangle, \\ |0,0\rangle_{+1} &= d_{+1\uparrow}^\dagger d_{+1\downarrow}^\dagger |0\rangle, \\ |0,0\rangle_0 &= \frac{1}{\sqrt{2}} \left( d_{+1\uparrow}^\dagger d_{-1\downarrow}^\dagger - d_{+1\downarrow}^\dagger d_{-1\uparrow}^\dagger \right) |0\rangle. \end{aligned}$$

These states are the eigenstates of the Hamiltonian (1) with  $|0,0\rangle_{-1}$  being the singlet state of the lowest energy. However, (1) is oversimplified by the assumption of the validity of the Random Matrix Theory [16]. In a more general model electron-electron interactions yield non-zero matrix elements

$${}_n\langle 0,0 | H_{dot} | 0,0 \rangle_{n'} \neq 0$$

for  $n \neq n'$ . As the result, the lowest energy singlet  $|0,0\rangle$  is no longer  $|0,0\rangle_{-1}$ , but a certain mixture of all 3 states  $|0,0\rangle_n$ :

$$|0,0\rangle = \sum_{n=0,\pm 1} C_n |0,0\rangle_n. \quad \sum_n C_n^2 = 1$$

This generalization of the dot's Hamiltonian yields additional coupling constants in the dot-lead exchange interaction. It turns out that such an extended model is identical to Eq. (21) as far as the low-temperature properties of the system are concerned. We demonstrate it on a specific example [12,13]:

$$C_0 = 0, \quad C_n = \frac{n}{\sqrt{2}} (-\cos \alpha + n \sin \alpha),$$

The case considered in [12,13] corresponds to  $\alpha = 0$  (or  $C_{-1} = -C_1 = 1/\sqrt{2}$ ). The choice of the singlet state in [11] and in Eq. (3) above corresponds to  $\alpha = \pi/4$  (or  $C_{-1} = 1, C_1 = 0$ ).

Of course, the transitions between the state  $|0,0\rangle$  and the triplet states  $|1, S^z\rangle$  can be described again in terms of 2 fictitious spin-1/2 operators  $\mathbf{S}_{1,2}$ . But instead of (17)-(18) we have now

$$\begin{aligned} \mathcal{P} \sum_{ss'} d_{ns}^\dagger \frac{\sigma_{ss'}}{2} d_{n's'} \mathcal{P} &= \frac{1}{2} \delta_{n,n'} \mathbf{S}_+ \\ &+ \frac{1}{2} \delta_{n,-n'} (\mathbf{S}_- \cos \alpha + 2in\mathbf{T} \sin \alpha), \\ \mathcal{P} \sum_s d_{ns}^\dagger d_{n's} \mathcal{P} &= n \delta_{n,n'} [(\mathbf{S}_1 \cdot \mathbf{S}_2) \sin(2\alpha) - 1/4 + n] \end{aligned}$$

Accordingly, the effective Hamiltonian also modifies: Eq. (20) remains unchanged while Eq. (21) is replaced by

$$\begin{aligned} H_n &= J(\mathbf{s}_{nn} \cdot \mathbf{S}_+) + V' n \rho_{nn} (\mathbf{S}_1 \cdot \mathbf{S}_2) \\ &+ \frac{I_S}{\sqrt{2}} (\mathbf{s}_{-n,n} \cdot \mathbf{S}_-) + \frac{I_T}{\sqrt{2}} 2in (\mathbf{s}_{-n,n} \cdot \mathbf{T}). \end{aligned} \quad (C1)$$

The coupling constants here are expressed through  $J, I, V$  of Eq. (23) as

$$I_S = I\sqrt{2} \cos \alpha, \quad I_T = I\sqrt{2} \sin \alpha, \quad V' = V \sin 2\alpha$$

[ $J$  is the same as in (23)].

The scaling equations for this Hamiltonian read

$$\begin{aligned} dJ/d\mathcal{L} &= \nu [J^2 + (I_S^2 + I_T^2)/2] \\ dI_S/d\mathcal{L} &= 2\nu (I_S J + I_T V') \\ dI_T/d\mathcal{L} &= 2\nu (I_T J + I_S V') \\ dV'/d\mathcal{L} &= 2\nu I_S I_T \end{aligned} \quad (C2)$$

(these equations are equivalent to Eqs. (17)-(20) of [12]). For  $\alpha \neq 0$  the initial values of all coupling constants differ from zero. System of equations (C2) allows for a solution in which all the coupling constants diverge at a certain point  $\mathcal{L} = \mathcal{L}_0$ . Similar to the conventional Kondo problem, the leading divergency is  $J, I_S, I_T, V' \propto (\mathcal{L}_0 - \mathcal{L})^{-1}$ . Examination of the subleading terms allows us to conclude that the solutions of (C2) and (27) coincide near this point if one sets  $I_S = I_T = I$  and  $V' = V$ . Indeed, it follows from the second and the third equations in (C2) that

$$\frac{d}{d\mathcal{L}} \ln(I_-/I_+) = -2\nu V', \quad I_\pm = \frac{1}{2}(I_S \pm I_T) \quad (C3)$$

Using the leading term of the asymptote of  $V'$ ,

$$1/\nu V' = (2/\zeta) (\mathcal{L}_0 - \mathcal{L}), \quad \zeta > 0,$$

and Eq. (C3) we find  $I_-/I_+ \propto (\mathcal{L}_0 - \mathcal{L})^\zeta$ . Therefore, in the vicinity of the point  $\mathcal{L}_0$  the difference between  $I_S$  and  $I_T$  can be neglected, and the resulting equations for  $J, I_+, V'$  coincide with Eqs. (27) for  $J, I, V$ .

So far we found a solution near some singularity point  $\mathcal{L} = \mathcal{L}_0$ . We should check now that such point is reached indeed by solutions satisfying the proper initial conditions at  $\mathcal{L} = 0$ . We were only able to perform this check by solving numerically the system (C2). Numerical solution for a set of models defined by  $\alpha$  in the interval  $0.01\pi \leq \alpha \leq \pi/4$  indeed verified the proper divergency of the coupling constants. We have also found that the

parameter  $c$  in Eq. (28) approaches  $1/2$  at small  $\alpha$ . In other words, in the limit  $\alpha \rightarrow +0$  the difference between  $T_0$  and  $T_K^{\text{dd}}$  disappears.

The convergence of the system of equations (C2) to Eqs. (27) means that the results of the main text are not sensitive to the details of intradot interactions. In particular, Eq.(37) with  $\lambda$  given by (32) holds.

We now consider the *special case*  $\alpha = 0$ , in which the exponent  $\lambda$  turns out to be different. We consider a slight generalization of the model, allowing for the dependence of the tunneling amplitudes on the orbital index:  $t_\alpha$  in Eq. (8) is replaced by  $t_{\alpha n}$ ; see also Appendix E). [Note that for  $\alpha \neq 0$  this extension does not affect the value of  $\lambda$  in Eq. (32)]. The exchange Hamiltonian for such model,

$$H_n = J_n(\mathbf{s}_{nn} \cdot \mathbf{S}_+) + I(\mathbf{s}_{-n,n} \cdot \mathbf{S}_-), \quad (\text{C4})$$

acquires an  $n$ -dependent exchange constant. The scaling equations in this case,

$$\frac{dJ_n}{d\mathcal{L}} = \nu(J_n^2 + I^2), \quad \frac{dI}{d\mathcal{L}} = \nu I \sum_n J_n, \quad (\text{C5})$$

have first integral

$$(J_{+1} - J_{-1})/2I = \tan \varphi, \quad |\varphi| < \pi/2.$$

The value of  $\varphi$  is determined by the bare value of the exchange constants. The first integral allows one to solve the scaling equations (C5) exactly [12,13]. Near the singularity point  $\mathcal{L}_0$  the solutions acquire asymptotic form

$$\nu J_n = \frac{1 + n \sin \varphi}{2(\mathcal{L}_0 - \mathcal{L})}, \quad \mathcal{L}_0 = \ln(\delta/T_0). \quad (\text{C6})$$

At the triplet side of the transition at energies below  $|K| \gg T_0, E_Z$  the system is described by the Hamiltonian (34) with  $n$ -dependent exchange amplitudes  $J_n$ . In this situation one can define two separate scales,  $T_n$ , corresponding to the two exchange constants,

$$T_n = |K| \exp[-1/\nu J_n(\mathcal{L}^*)], \quad \mathcal{L}^* = \ln(\delta/|K|).$$

At these scales the two exchange constants,  $\nu J_n$ , become of the order of 1. Substitution here of  $J_n(\mathcal{L})$  from Eq. (C6) then yields

$$\frac{T_n}{T_0} = \left( \frac{T_0}{|K|} \right)^{\lambda_n}, \quad \lambda_n(\varphi) = \frac{1 - n \sin \varphi}{1 + n \sin \varphi}.$$

The larger of the two scales corresponds to the smallest of the two exponents  $\lambda_n$  [12], [13]:

$$\min \lambda_n = \frac{1 - \sin |\varphi|}{1 + \sin |\varphi|} < 1.$$

The Hamiltonian (C4) formally coincides with that for the two impurity Kondo model [22], see Eq. (26) above.

If  $J_n$  do not depend of  $n$ , this model exhibits an exotic non-Fermi liquid behavior [22]. Note that the non-Fermi liquid state is extremely fragile and is also destroyed by potential scattering, which we have neglected in our derivation. The requirements  $\alpha = 0$  and  $\varphi = 0$  set strict conditions on both the intradot interaction constants and on the values of the tunneling amplitudes. Finding these conditions is beyond the scope of the present paper.

## APPENDIX D: THE EFFECTIVE EXCHANGE HAMILTONIAN FOR THE CASE OF ORBITAL MIXING

In order to see how our results are modified in the case when the orbital mixing is allowed in the course of tunneling, we choose the tunneling amplitudes in Eq. (7) in the form

$$t_{\alpha nm} = t_\alpha \delta_{n,m} + t'_\alpha \delta_{n,-m}, \quad \alpha = R, L \quad (\text{D1})$$

The rotation in the orbital space,

$$c_{\alpha nks} = \frac{1}{\sqrt{2}} (\tilde{c}_{\alpha nks} - n \tilde{c}_{\alpha -nks}),$$

$$d_{ns} = \frac{1}{\sqrt{2}} (\tilde{d}_{ns} - n \tilde{d}_{-ns})$$

diagonalizes  $H_T$ :

$$H_T = \sum_{\alpha n} v_{\alpha n} \tilde{c}_{\alpha nks}^\dagger \tilde{d}_{ns} + \text{H.c.}, \quad v_{\alpha n} = t_\alpha + n t'_\alpha$$

and modifies Eqs. (17),(18). Next, we perform a rotation in the  $R - L$  space, similar to (9)

$$\begin{pmatrix} \psi_{nks} \\ \phi_{nks} \end{pmatrix} = \frac{1}{\sqrt{v_{Ln}^2 + v_{Rn}^2}} \begin{pmatrix} v_{Rn} & v_{Ln} \\ -v_{Ln} & v_{Rn} \end{pmatrix} \begin{pmatrix} \tilde{c}_{Rnks} \\ \tilde{c}_{Lnks} \end{pmatrix},$$

which yields

$$H_T = \sum_{nks} v_n \psi_{nks}^\dagger \tilde{d}_{ns} + \text{H.c.}, \quad v_n^2 = v_{Ln}^2 + v_{Rn}^2,$$

We now perform a Schrieffer-Wolff transformation, which yields Eq. (20) with  $H_n$  given by

$$H_n = J_n(\mathbf{s}_{n,n} \cdot \mathbf{S}_+) + I_n \frac{n}{\sqrt{2}} (\mathbf{s}_{n,n} \cdot \mathbf{S}_-) + I\sqrt{2}in(\mathbf{s}_{-n,n} \cdot \mathbf{T}) - V\rho_{-n,n}(\mathbf{S}_1 \cdot \mathbf{S}_2). \quad (\text{D2})$$

The scaling equations for this model read

$$\begin{aligned} dJ_n/d\mathcal{L} &= \nu [J_n^2 + (I_n^2 + I^2)/2] \\ dI_n/d\mathcal{L} &= 2\nu (IV + J_n I_n) \\ dI/d\mathcal{L} &= \nu \sum_n (I J_n + V I_n) \\ dV/d\mathcal{L} &= \nu \sum_n I I_n \end{aligned} \quad (\text{D3})$$

In a generic case  $t_\alpha \neq t'_\alpha$  the initial values of all the coupling constants in (D3) are finite:

$$J_n = I_n = 2v_n^2/E_C, \quad I = 2V = 2v_{+1}v_{-1}/E_C.$$

For example, for

$$t'_\alpha/t_\alpha = \beta \quad (\text{D4})$$

one obtains

$$J_n = I_n = (1 + n\beta)^2 J_0, \quad I = 2V = (1 - \beta^2) J_0,$$

where  $J_0 = 2(t_L^2 + t_R^2)/E_C$ .

System of equations (D3) allows for a solution in which all the coupling constants diverge at a certain point  $\mathcal{L} = \mathcal{L}_0$ , with the leading divergency being of the form  $J_n, I_n, I, V \propto (\mathcal{L}_0 - \mathcal{L})^{-1}$ . The analysis of the subleading terms similar to that in Appendix C leads to a conclusion that in the vicinity of the point  $\mathcal{L}_0$  the difference between  $J_{+1}$  and  $J_{-1}$ , and the difference between  $I_n$  and  $I$  can be neglected. The resulting equations are identical to Eqs. (27). Accordingly, near the point  $\mathcal{L}_0$  the solutions of Eqs. (D3) coincide with that of Eqs. (31) if  $J_n = J$  and  $I_n = I$ . Note that setting  $J_n = J$  and  $I_n = I$  in Eq. (D2) and performing a unitary transformation

$$\psi_{nks} = \frac{1}{\sqrt{2}} (a_{nks} + na_{-nks})$$

brings the exchange Hamiltonian (D2) to the form (21).

We solved Eqs. (D3) numerically for  $\beta$  [see Eq. (D4)] in the interval  $0 \leq \beta \leq 0.9$  (note that for the model defined by Eqs. (D1) and (D4) all physical observables possess a symmetry with respect to the change  $\beta \rightarrow 1/\beta$ ). These calculations confirmed that the proper divergency of the coupling constants indeed occurs.

It turns out that the relation between  $T_K^{\text{triplet}}$  and  $T_K^{\text{odd}}$  (see Section IV) depends on the degree of orbital mixing: the stronger the orbitals are mixed the less the difference between  $T_K^{\text{triplet}}$  and  $T_K^{\text{odd}}$  is. For example, for the model (D1),(D4)  $T_K^{\text{triplet}}$  can be associated with the larger of the two energy scales  $T_n = \delta \exp(-1/\nu J_n)$ , while  $T_K^{\text{odd}} = \delta \exp(-1/\nu J_{\text{odd}})$  with  $J_{\text{odd}} = 2(1 + \beta^2)J_0$ . This yields

$$\frac{\ln(\delta/T_K^{\text{triplet}})}{\ln(\delta/T_K^{\text{odd}})} = 2 \frac{1 + \beta^2}{(1 + \beta)^2}.$$

The expression in the r.h.s. here is invariant with respect to the change  $\beta \leftrightarrow 1/\beta$  and its value varies between 2 for  $\beta = 0$  (or  $\beta = \infty$ ) and 1 for  $\beta = 1$ . Therefore, the temperature scales  $T_K^{\text{triplet}}$  and  $T_K^{\text{odd}}$  coincide in the strong mixing limit  $\beta \rightarrow 1$ . The experiments with vertical quantum dots [7] correspond to  $T_K^{\text{triplet}} \ll T_K^{\text{odd}}$ , which can be explained only if the mixing is weak ( $\beta \ll 1$  or  $1/\beta \ll 1$ ).

Note that the relation between  $T_0$  and  $T_K^{\text{odd}}$  depends on  $\beta$  much weaker. For instance, for  $\beta = 1$  the ratio

$$\frac{\ln(\delta/T_0)}{\ln(\delta/T_K^{\text{odd}})} = \frac{1}{1 + 1/\sqrt{2}} \approx 0.6,$$

while for  $\beta = 0$  this ratio equals approximately 0.7, see Eqs. (28) and (30). Accordingly, for  $\delta \gg T_0$  the inequality  $T_0 \gg T_K^{\text{odd}}$  holds independently of the strength of the orbital mixing.

## APPENDIX E: TWO-STAGE KONDO EFFECT

In this Appendix, we consider an example of the non-universal features that the system may exhibit far away from the transition point. Consider the following generalization of (8):

$$t_{\alpha nn'} = t_{\alpha n} \delta_{nn'}. \quad (\text{E1})$$

After a rotation in the left-right space

$$\begin{pmatrix} \psi_{nks} \\ \phi_{nks} \end{pmatrix} = \frac{1}{t_n} \begin{pmatrix} t_{Rn} & t_{Ln} \\ -t_{Ln} & t_{Rn} \end{pmatrix} \begin{pmatrix} c_{Rnks} \\ c_{Lnks} \end{pmatrix}, \quad t_n^2 = t_{Ln}^2 + t_{Rn}^2$$

and a Schrieffer-Wolff transformation one obtains Eqs. (20)-(21) with  $J$  and  $V$  in (21) replaced by  $J_n$  and  $V_n$ ,

$$J_n = 2V_n = 2t_n^2/E_C, \quad I = 2t_{+1}t_{-1}/E_C.$$

This is only a small modification as far as the vicinity of the singlet-triplet transition is concerned. Indeed, the scaling equations (27) are replaced by

$$\begin{aligned} dJ_n/d\mathcal{L} &= \nu (J_n^2 + I^2), \\ dI/d\mathcal{L} &= \nu I \sum_n (J_n + V_n), \\ dV_n/d\mathcal{L} &= 2\nu I^2 \end{aligned}$$

If these equations are rewritten in terms of new variables

$$\begin{aligned} J &= (J_{+1} + J_{-1})/2, \quad V = (V_{+1} + V_{-1})/2, \\ J' &= (J_{+1} - J_{-1})/2, \quad V' = (V_{+1} - V_{-1})/2, \end{aligned}$$

one finds that  $J, I$ , and  $V$  behave at large  $\mathcal{L}$  according to Eq. (31), all being proportional to  $(\mathcal{L}_0 - \mathcal{L})^{-1}$ , while  $J'$  diverges much slower, as  $J' \propto (\mathcal{L}_0 - \mathcal{L})^{-2/(\lambda+1)}$ , and  $V'$  is not renormalized at all.

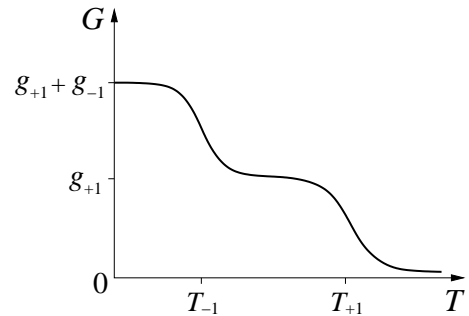


FIG. 5. Staircase-like temperature dependence of the linear conductance at the triplet side of the singlet-triplet transition.

Interesting properties appear at the triplet side of the transition in the case when the exchange constants are very different, say,  $J_{+1} \gg J_{-1}$ .

The exchange term in the Hamiltonian (34) is replaced by  $\sum_n J_n (\mathbf{s}_{nn} \cdot \mathbf{S})$ . One can define two separate Kondo temperatures

$$T_n = \delta \exp(-1/\nu J_n), \quad T_{+1} \gg T_{-1}$$

corresponding to the two exchange constants  $J_n$ . At  $T \gg T_{+1} \gg T_{-1}$  the presence of the  $n = -1$  channel can be neglected, so that the system in this regime is described by a single-channel  $S = 1$  Kondo model. Accordingly, the conductance in this regime is given by

$$G = g_{+1} \frac{\pi^2/2}{[\ln(T/T_{+1})]^2}, \quad T \gg T_{+1} \quad (\text{E2})$$

where  $g_n = (2e^2/h) 4t_{Ln}^2 t_{Rn}^2 t_n^{-4}$ . At  $T \ll T_{+1}$  the scattering in the  $n = +1$  channel reaches the unitary limit. In this regime one half of the dot's spin is screened [21]. The remaining spin  $S = 1/2$  still interacts with the electron continuum in the channel  $n = -1$ . This antiferromagnetic exchange coupling eventually results in the second stage of the Kondo effect. The corresponding asymptote of the conductance is

$$G = g_{+1} + g_{-1} \frac{3\pi^2/16}{[\ln(T/T_{-1})]^2}, \quad T_{-1} \ll T \ll T_{+1} \quad (\text{E3})$$

At  $T \ll T_{-1}$  the dot's spin is screened entirely [21]. The zero-temperature conductance  $G_0 = g_{+1} + g_{-1}$ ; the leading finite temperature correction  $G_0 - G \propto (T/T_{-1})^2$ .

Equations (E2) and (E3) describe a staircase-like temperature dependence of the conductance, see Fig. 5. The thermodynamic quantities are expected to exhibit a similar two-stage crossover [27].

---

[1] L. P. Kouwenhoven, C. M. Marcus, P. L. McEuen, S. Tarucha, R. M. Westervelt, and N. S. Wingreen, in *Mesoscopic Electron Transport*, eds. L. L. Sohn, L.P. Kouwenhoven, and G. Schön, NATO ASI Series E – vol. 345 (Kluwer, Dordrecht, 1997) pp. 105-214.

[2] C. B. Duke, *Tunneling in Solids* (Academic Press, New York, 1969); J. M. Rowell, in *Tunneling Phenomena in Solids*, edited by E. Burstein and S. Lundqvist (Plenum, New York, 1969).

[3] A. F. G. Wyatt, Phys. Rev. Lett. **13**, 401 (1964); R. A. Logan and J. M. Rowell, Phys. Rev. Lett. **13**, 404 (1964).

[4] J. Appelbaum, Phys. Rev. Lett. **17**, 91 (1966); Phys. Rev. **154**, 633 (1967); P. W. Anderson, Phys. Rev. Lett. **17**, 95 (1966).

[5] J. Kondo, Prog. Theor. Phys. **32**, 37 (1964).

[6] D. Goldhaber-Gordon, H. Shtrikman H, D. Mahalu, D. Abusch-Magder, U. Meirav, M. A. Kastner, Nature (London) **391**, 156 (1998); S. M. Cronenwett, T. H. Oosterkamp, and L. P. Kouwenhoven, Science **281**, 540 (1998); J. Schmid, J. Weis, K. Eberl, K. v. Klitzing, Physica (Amsterdam) **256B-258B**, 182 (1998).

[7] S. Sasaki, S. De Franceschi, J. M. Elzerman, W. G. van der Wiel, M. Eto, S. Tarucha, and L. P. Kouwenhoven Nature **405**, 764 (2000).

[8] J. Schmid, J. Weis, K. Eberl, K. v. Klitzing, Phys. Rev. Lett. **84**, 5824 (2000).

[9] J. Nygård, D. H. Cobden, and P. E. Lindelof, Nature, **408**, 342 (2000).

[10] M. Pustilnik, L. I. Glazman, D. H. Cobden, and L. P. Kouwenhoven, cond-mat/0010336.

[11] M. Pustilnik and L. I. Glazman, Phys. Rev. Lett. **85**, 2993 (2000).

[12] M. Eto and Yu. V. Nazarov, Phys. Rev. Lett. **85**, 1306 (2000).

[13] M. Eto and Yu. V. Nazarov, cond-mat/0101152.

[14] S. Tarucha, D.G. Austing, Y. Tokura, W. G. van der Wiel, and L. P. Kouwenhoven, Phys. Rev. Lett. **84**, 2485 (2000); L. P. Kouwenhoven, T. H. Oosterkamp, M. W. S. Danoesastro, M. Eto, D. G. Austing, T. Honda, S. Tarucha, Science **278**, 1788 (1997); D.G. Austing, S. Sasaki, S. Tarucha, S. M. Reimann, M. Koskinen, M. Manninen, Phys. Rev. B **60**, 11514 (1999).

[15] M. Pustilnik, Y. Avishai, and K. Kikoin, Phys. Rev. Lett. **84**, 1756 (2000).

[16] I. L. Kurland, I. L. Aleiner, and B. L. Altshuler, Phys. Rev. B **62**, 14886 (2000).

[17] L. I. Glazman and M. E. Raikh, JETP Lett. **47**, 452 (1988); T. K. Ng and P. A. Lee, Phys. Rev. Lett. **61**, 1768 (1988).

[18] P. W. Brouwer, X. Waintal, and B. I. Halperin, Phys. Rev. Lett. **85**, 369 (2000); K. A. Matveev, L. I. Glazman, and A. I. Larkin, Phys. Rev. Lett. **85**, 2789 (2000).

[19] A. M. Tsvelick and P. B. Wiegmann, Adv. Phys. **32**, 453 (1983).

[20] T. Inoshita *et al.*, Phys. Rev. B **48**, 14725 (1993); L. I. Glazman, F. W. Hekking, and A. I. Larkin, Phys. Rev. Lett. **83**, 1830 (1999); A. Kaminski and L. I. Glazman, Phys. Rev. B **61**, 15297 (2000); I. L. Aleiner, P. W. Brouwer, and L. I. Glazman, cond-mat/0103008.

[21] P. Nozières and A. Blandin, J. Physique **41**, 193 (1980).

[22] I. Affleck, A. W. W. Ludwig, and B. A. Jones, Phys. Rev. B **52**, 9528 (1995); A. J. Millis, B. G. Kotliar, and B. A. Jones, in *Field Theories in Condensed Matter Physics*, edited by Z. Tesaovic (Addison Wesley, Redwood City, CA, 1990), pp. 159-166.

[23] P. W. Anderson, J. Phys. C **3**, 2436 (1970).

[24] P. Nozières, J. Low Temp. Phys. **17**, 31 (1974).

[25] T. A. Costi, A. C. Hewson, and V. Zlatić, J. Phys. CM **6**, 2519 (1994); T. A. Costi, Phys. Rev. Lett. **85**, 1504 (2000).

[26] G. Burkard, D. Loss, and D. P. DiVincenzo, Phys. Rev. B **59**, 2070 (1999).

[27] N. Andrei and A. Jerez, Phys. Rev. Lett. **74**, 4507 (1995).